GaAs TUNNETT Diodes

JUN-ICHI NISHIZAWA, FELLOW, IEEE, KAORU MOTOYA, STUDENT MEMBER, IEEE, AND YASUO OKUNO

Abstract—**The tunnel-injection-transit-time (TUNNETT) diode is operated at a high frequency and has a low-noise level compared to the IMPATT diode. The tunnel injection in a thin carrier generating region of the TUNNETT depends strongly on the electric-field intensity over 1000 kV/cm where the ionization of carriers can be neglected, leading to a higher efficiency performance than that of the IMPATT. GaAs TUNNETT diodes with p^+-n and p^+-n-n^+ structures have been fabricated by a new LPE method (the temperature-difference method under controlled vapor pressure). The fundamental oscillation at frequencies from about 100 up to 248 GHz has been obtained from the pulse-driven p^+-n-n^+ diodes. This paper describes the details of the oscillation characteristics of GaAs TUNNETT diodes.**

I. Introduction

In 1958, the tunnel-injection-transit-time (TUNNETT) diode was proposed by Nishizawa and Watanabe [1]. The concept of this diode was introduced in the analysis of the high-frequency properties of the avalanching-negative-resistance diode which today is called the IMPATT diode. A further reduction in the length of the transit-time-negative-resistance (TTNR) region of the TTNR diode realizes a still higher oscillation frequency. At the same time, for the high-frequency oscillation, the tunnel effect becomes important as the mechanism of the injection for the TTNR diode at short-millimeter to submillimeter wavelengths. The tunnel injection dominates, as an example, with an electric field over 1000 kV/cm for the length of a tunneling injection region of approximately less than 100 Å in a reverse-biased p-n junction. Therefore, the major advantages of the TUNNETT over the IMPATT are the low noise and low-bias voltage as the respects of the fundamental properties of tunneling; moreover, because of the lower dispersion effect in the tunneling injection, which will be described below, f_{max} of the TUNNETT has been estimated to be about 1000 GHz [2].

The length of the avalanche region cannot be decreased, because the region for avalanche injection requires a certain value for the length and the time to produce enough carriers, which has been understood to help the time-delay effect. Recently Nishizawa *et al.* published the analysis of this phenomenon, which has been understood to be a simple time-delay phenomenon, defining it as the avalanche-induced dispersion effect [3]. This leads to the reduction of the amplitude of the injected carriers when a higher frequency voltage is applied to the TTNR diode, finally, the operation of the so-called impact ionization transit-time mode is limited. Moreover, the ionization coefficients of the electron and hole and their derivatives, with respect to the electric-field intensity, saturate at a high field below 1000 kV/cm [4]; however, the increase of the applied field intensity for the avalanche injection region does not help to keep the amount of amplitude of the generated carriers in the shortened length of the avalanche region. Thus the efficiency of the IMPATT decreases progressively.

The tunnel injection region is a strong function of the electric field over 1000 kV/cm, because it is very easy to obtain a higher amplitude of injection and because it is very useful due to its very small time constant as compared to that of the avalanche injection. Moreover, since the tunnel injection is independent of the dispersion effect, the injection into the transit-time region of the TUNNETT can be much stronger. The length of the TTNR region however, should be designed to be much thicker than that in the IMPATT diode to compensate for the shorter time delay in the injection region; nevertheless, the performance efficiency in the TUNNETT still will be much higher than that of the IMPATT in a high-frequency region because of the lower dispersion in the injection region. Hence the TUNNETT will be useful in the range from the short-millimeter to submillimeter wave.

Since the experimental confirmation of the TUNNETT oscillation fabricated from the GaAs p-n diodes in 1968 by Nishizawa *et al.*, concentrated research efforts on device improvements have been carried out [5]–[9].

This paper describes the GaAs diodes fabricated by a new LPE method (TDM under CVP) [10] to be capable up to 248-GHz oscillations; in addition, consideration is given to the design of the TUNNETT and details of the pulsed-oscillation characteristics of the GaAs TUNNETT diodes with p^+-n and p^+-n-n^+ structures.

II. Design

It is well known that the breakdown mechanism changes from avalanche to tunnel injection in a reverse-biased p-n diode when the doping level of impurities increases. As this tunnel injection is used in this diode, it can be said that the TUNNETT is not a minority carrier device like the BARITT but a majority carrier device like the IMPATT. The TUNNETT has an unfavorable in-phase injection like the BARITT and, consequently, a corresponding larger transit angle is needed for negative resistance in contrast to the IMPATT. This inherent dis-

Manuscript received May 29, 1978; revised August 4, 1978.

J. I. Nishizawa and K. Motoya are with the Research Institute of Electrical Communications, Tohoku University, Sendai 980, Japan.

Y. Okuno is with the Semiconductor Research Institute, Kawauchi, Sendai 980, Japan.

0018-9480/78/1200-1029$00.75 ©1978 IEEE

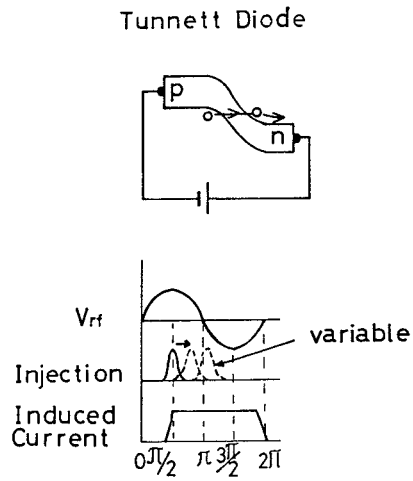

Fig. 1. Operating principle of the TUNNETT diode.

TABLE I
ESSENTIAL FEATURES OF THE TUNNET DIODE AND THE IMPATT DIODE

	Tunnett	Impatt
f_{max} of the fundamental oscillation frequency(GHz)	~ 1000GHz	90GHz*
Electric field intensity (kV/cm)	>1000	<1000
Bias voltage	small	higher than the Tunnett
Noise level	small	high
Temperature coefficient	negative	positive

*[17].

advantage may be useful only at very high frequencies. However, the avalanche-induced dispersion effect in the IMPATT [3], [11] causes the carrier dispersion but not the time delay, so the magnitudes of avalanche-injected carriers disperse spacially. This effect will be effective on the degradation in the performance of the IMPATT even at low frequencies; consequently, the TUNNETT will be useful above the short-millimeter-wave region.

The essential features of the TUNNETT are shown in Table I. The features of high-frequency capability, low applied-voltage operation, and low noise will be attractive for practical application. Several structures of the TUNNETT such as a reverse-biased p-n diode, a reverse-biased Schottky-barrier diode, or a MIS diode have been proposed [2]. Among them, the p-n diode probably exhibits the better performance because of its higher injection efficiency and excellent thermal stability. For the p-n diodes, various structures such as p^+-n, p^+-n-n^+, and p^+-n-ν-n^+ can be considered. In addition, both types with the single-drift region (SDR) and the double-drift region (DDR) will be available for the TUNNETT.

The operating principle of the p-n TUNNETT is shown in Fig. 1. When the maximum injection at $\pi/2$ rad is assumed, the optimum transit angle will be $3\pi/2$ rad, which is much thicker than that in the IMPATT, and it makes it much easier to prepare the diode for high-

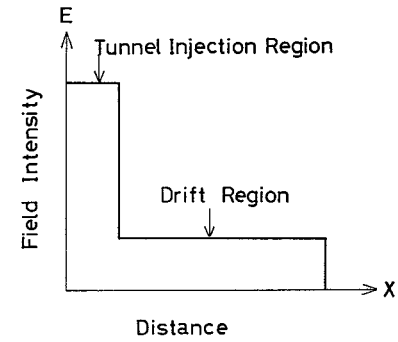

Fig. 2. Ideal electric-field distribution of the TUNNETT diode.

frequency application. Then the width of the transit region is given by

$$W_d = \frac{3v_s}{4f} \tag{1}$$

where v_s is the saturated velocity of carriers and f is the operating frequency.

However, the injection phase is allowed to be varied to a value larger than $\pi/2$ rad by controlling the time constant which charges up the tunneling junction in the actual operation. This means that the concentration of the field intensity in the tunneling region needs a certain time to ionize impurities in the depletion layer of the tunneling junction. The electric-field distribution in the diode should be designed to achieve the optimum injection efficiency [2], [9]. The field distribution as shown in Fig. 2 consists of the localized thin tunnel injection region with a high field intensity and the drift region with a relatively low field intensity enough to maintain the saturation velocity of the injected carriers. The high resistive layer will be required for the drift region in order to build enough field intensity even with very low current. With regard to this viewpoint, the p^+-n^+-ν-n^+ structure is suitable to realize the efficient TUNNETT diode. However, in the diodes used in this experiment, the resistivity in the drift region is not enough; the field is cut by the ohmic-voltage drop which needs a higher current flow for the field intensity in order to oscillate, and this is believed to be the cause of the relatively lower efficiency of the diode.

The tunnel injection current of a reverse-biased p-n diode is determined by the physical parameters of materials including the band structure, band gap, and effective mass of the electron and hole. Moreover, the upper limit of the operating frequency in the TTNR diode is determined by the diffusion process of the injected carriers [1]. The materials for diode fabrication which exhibit the ready availability of the tunneling effect, a higher saturated velocity, a lower diffusion coefficient of the carriers, and a higher thermal conductivity are essential for the realization of the TUNNETT operating higher frequency region. The preparation of crystals with good crystallographic quality, accurate control of the doping profile of the junction, and microfabrication technology are also necessary, since the high electric field and current density should be applied to the junction.

III. Material Preparation and Device Fabrication [9]

GaAs diodes are fabricated from the epitaxial wafer grown by the temperature-difference method (TDM) under controlled vapor pressure (CVP). The n- or n-n^+-type layers are grown on the (100) Zn doped p^+-type substrate ($\rho: 4 \sim 6 \times 10^{-3}\,\Omega\cdot$cm) and the growth temperature ranges from 600 to 700° C in order to prevent Zn diffusion into the n layer. Special care is taken during the wafer thinning process and the formation of ohmic contacts to the n- (or n^+-) and the p^+-type layer [12]. The structure of a p^+-n-n^+ diode and the properties of the epitaxially grown wafers are shown in Table II.

Prior to the oscillation experiment, the static C-V and the I-V characteristics have been measured. The $1/C^2$-V plots of the p^+-n-n^+ diode fabricated from three different wafers are shown in Fig. 3. This data shows that an abrupt impurity distribution has successfully formed in the junction, and the built-in voltage is about 1.3 V. The I-V characteristic of the p^+-n diode measured at various temperatures is shown in Fig. 4 together with the theoretically calculated lines. The direct tunnel current density in a p-n junction is given by the following equation [13], [14];

$$J_t = \frac{\sqrt{2}\, q^3 m^* V_a E}{4\pi^3 \hbar^2 \epsilon g^{1/2}} \exp\left(-\frac{\pi m^{*1/2} \epsilon g^{3/2}}{2\sqrt{2}\, qE\hbar}\right) \tag{2}$$

where E is the electric-field intensity in the junction, ϵg is the band gap energy, V_a is the applied voltage, and m^* is the reduced effective mass represented by [15]

$$m^* = \frac{1}{1/m_e^* + 1/m_{lh}^*} \tag{3}$$

where m_e^* is the electron effective mass and m_{lh}^* is the effective light hole mass. Approximating E by the peak field of the p^+-n (abrupt) junction, E is given by

$$E = \sqrt{\frac{2qN_D(V_a + V_b)}{\epsilon_0 \epsilon_s}} \tag{4}$$

where V_b is the built-in voltage of the junction, N_D is the donor density in the n layer, and ϵ_s is the dielectric constant of the material.

Substituting (4) into (2) yields

$$J_t = B_1 \sqrt{V_a + V_b}\; V_a \exp\left(-\frac{B_2}{\sqrt{V_a + V_b}}\right) \tag{5}$$

where

$$B_1 = \frac{q^3}{2\pi^3 \hbar^2} \sqrt{\frac{qm^* N_D}{\epsilon_0 \epsilon_s \epsilon g}} \tag{6}$$

and

$$B_2 = \frac{\pi \epsilon g}{4q\hbar} \sqrt{\frac{\epsilon_0 \epsilon_s \epsilon g m^*}{qN_D}}\,. \tag{7}$$

The experimental results of the I-V characteristic show that the current through the diode with $N_D \simeq 5 \times 10^{17}$

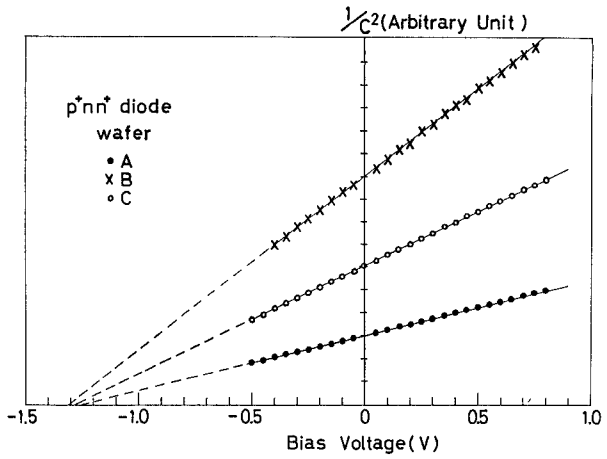

Fig. 3. $1/C^2$-V plots of the p^+-n-n^+ diodes fabricated from three different wafers.

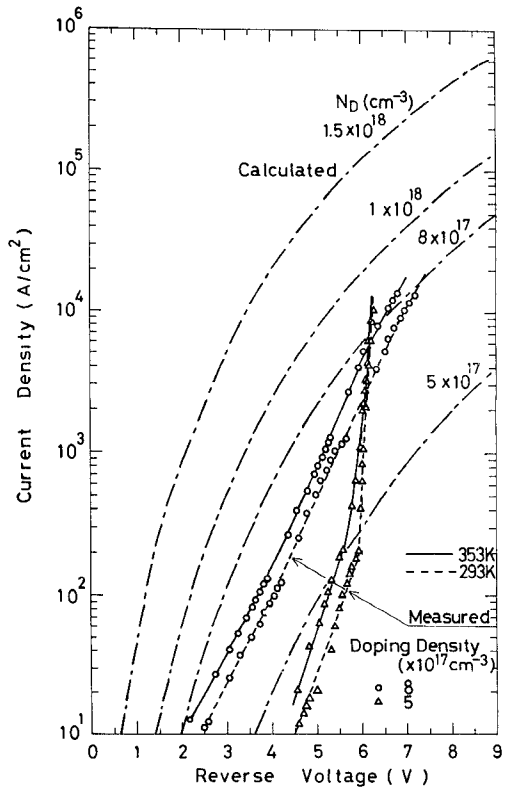

Fig. 4. I-V characteristics of the GaAs p^+-n diode. Calculated lines (—·—) are also indicated. ($\epsilon g = 1.43$ eV, $m_e^* = 0.068\ m_0$, $m_{lh}^* = 0.12\ m_0$, $\epsilon_s = 10.9$)

TABLE II
Structure of the p^+-n-n^+ Diode and the Properties of the Epitaxially Grown Wafers

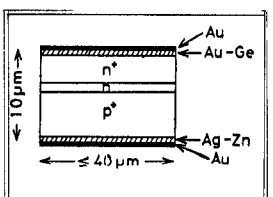

Diode Structure	Growth Temperature (°C)	Doping Density of n layer (cm^{-3})	Doping Density of n^+ layer (cm^{-3})	Thickness of n layer (μm)
p^+n	600 - 670	$5-10 \times 10^{17}$	——	1 - 2
$p^+n\,n^+$	640 - 650	1×10^{18}	$>3 \times 10^{18}$	0.7 - 3

cm^{-3} starts to flow abruptly at about -6 V. However, the I-V characteristic of the diode with $N_D \simeq 8\times10^{17}$ cm^{-3} seems to be nearly exponential over 10 A/cm^2, and there is no indication of an abrupt rise-up in current up to 10^4 A/cm^2. The calculated results of (5) show that a considerable amount of the tunneling current will flow into the diode with $N_D \geqslant 1\times10^{18}$ cm^{-3}. The temperature coefficient β of the I-V characteristic is assumed to be given by

$$\beta = \frac{\Delta V}{V_{293\,K}\Delta T} \tag{8}$$

where $\Delta V = V - V_{293\ K}$ and $\Delta T = T - 293$ K. The sign (negative or positive) of β is used to evaluate the injection mechanism in the junction. When the tunnel injection is dominant in the junction, β is negative. β of the p^+-n diode with $N_D \simeq 5\times10^{17}$ cm^{-3} is slightly negative or zero in the junction region, and β of the p^+-n (or p^+-n-n^+) diodes with $N_D \geqslant 8\times10^{17}$ cm^{-3} is negative as shown in Fig. 4. These results coincide with the previous ones [5] and is different from that of the Si diode where not direct but indirect tunneling occurs [16]. The fabricated GaAs diode with $N_D \geqslant 8\times10^{17}$ cm^{-3} is not an avalanche but a tunnel diode.

IV. Oscillation Experiment

A. Oscillator Circuit

The conventional quartz standoff structure diodes are positioned in T- (110~170 GHz), G- (140~220 GHz), Y- (170~260 GHz), and D-band (220~325 GHz) full-size rectangular waveguide cavities, and the oscillation frequency has been adjusted by changing the external circuit condition. The cross section of the TUNNETT diode mounted in the oscillator circuit is shown in Fig. 5. The diodes have been driven by a current pulse (50~100 ns and 50~100 Hz) through a bias post. The tuning is adjusted by the selection of the bias post and the short plunger so as to obtain the maximum output power. The output power is detected by a Si point-contact diode mounted in the T-band waveguide, and the oscillation frequency is measured by the voltage standing wave in the waveguide.

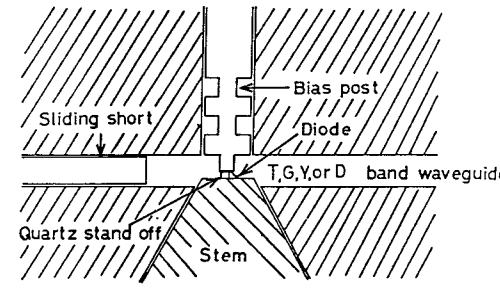

Fig. 5. Cross section of the TUNNETT diode oscillator circuit.

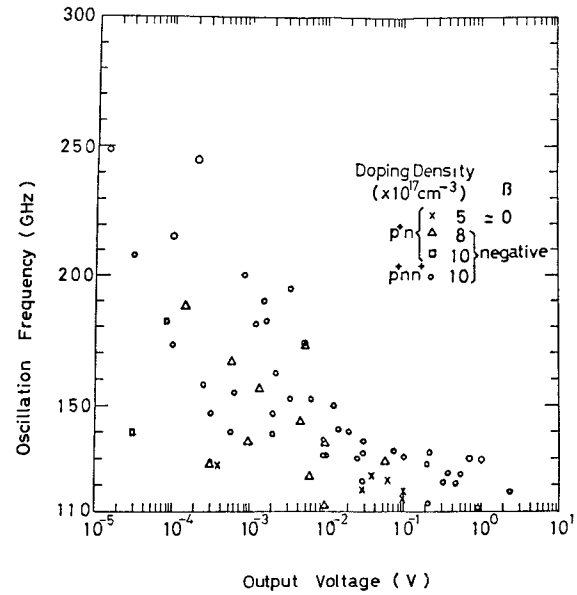

Fig. 6. The relation between the oscillation frequency and the output voltage of the detector of the p^+-n and p^+-n-n diode.

TABLE III
Parameters of the Oscillated Diodes

Diode Structure	Doping Density of n layer (cm^{-3})	β	V_{th} (V)	f_{max} (GHz)	E_{max} (kV/cm)
$p^+n\,n^+$	1×10^{18}	negative	-6.8 ~ -7.9	248	1600~1900
p^+n	5×10^{17}	≈ 0	-6.5 ~ -7.8	130	1150~1250
	$8\sim10\times10^{17}$	negative	-7 ~ -10	188	1400~1500

β: Temperature coefficient in I-V characteristics.
V_{th}: Threshold bias voltage for the oscillation.

B. Oscillation Performance

Table III summarizes the oscillated diodes. The lower doping diode exhibits a lower oscillation frequency among the diodes experimented. The relation between the oscillation frequency and the output voltage of the detector is shown in Fig. 6. The TUNNETT-mode oscillation from the diodes with $N_D \geqslant 8\times10^{17}$ cm^{-3} gives a wide range of fundamental oscillation frequency between about 100 and 248 GHz, while the performance of the diode with $N_D \simeq 5\times10^{17}$ cm^{-3} is inferior to that of the TUNNETT-mode oscillation. This comes from the fact that the electric-field intensity increases with an increase in the doping density of the n layer, and then the tunnel injection occurs more significantly. These results suggest that the TUNNETT oscillation can be obtained from the GaAs p^+-n or p^+-n-n^+ diode with $N_D \geqslant$ about 8×10^{17} cm^{-3} and the electric field in excess of about 1400~1500 kV/cm.

The relation between the bias current density (J_{dc}) and the oscillation frequency of the p^+-n-n^+ diodes fabricated from each of the two wafers is shown in Figs. 7(a) and (b). The diode oscillated at 248 GHz is mounted in the D-band cavity. The lowest J_{dc} obtained from the p^+-n-n^+ diode is about 8×10^4 A/cm^2 as shown in Fig. 7(a). To confirm the lower limit of the fundamental oscillation frequency, the p^+-n-n^+ diode (A) is mounted in the R-band (75~110-GHz) cavity with a cutoff frequency of 59 GHz. The diode with an area of 2.6×10^{-5} cm^2 oscillates from 95 to 102 GHz at the J_{dc} from 1.08 to 1.54×10^5

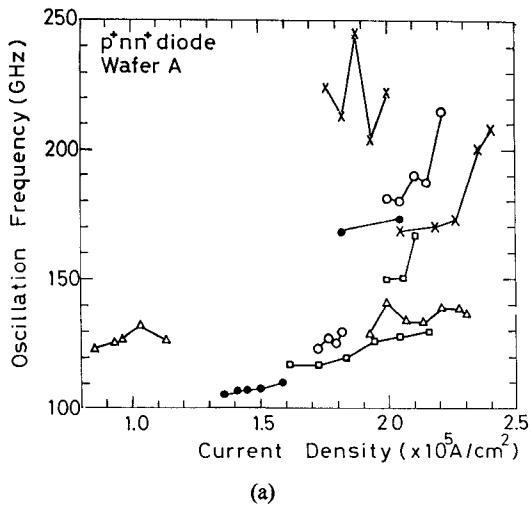

(a)

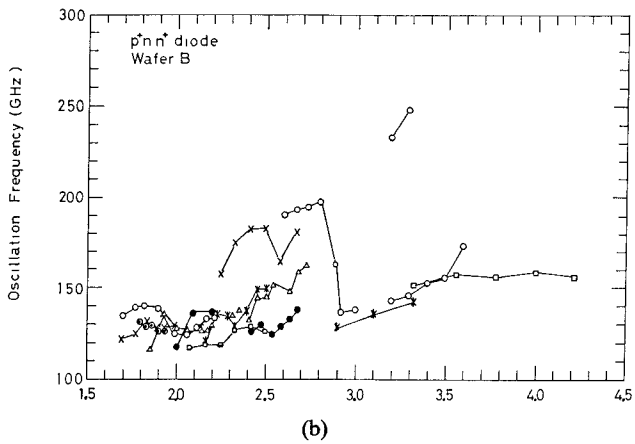

(b)

Fig. 7. Current density dependency of the oscillation frequency of the p^+-n-n^+ diode fabricated from (a) wafer *A* and (b) wafer *B*.

A/cm^2. Several diodes mounted in the *R*-band cavity oscillate only near the higher band edge of the *R* band, so that the fundamental oscillation frequency is assumed to start at about 100 GHz. Therefore, the oscillation obtained in our experiment is thought as the fundamental mode. These results are different from those of the Si IMPATT operating up to 400 GHz in the fifth harmonic mode. It is reported that the fundamental oscillation frequency ranges from 30 to 90 GHz. [17]

The measurement of the pulsed power level is being carried out using the Si point-contact diode. A thin-film thermocouple power detector (Anritzu model MP85B) and the CW source (190~210 GHz) consisting of a klystron and a doubler are used in the calibration of the detector. The experimental results assure that the output power of 1 mW can be realized for operation near 200 GHz.

The oscillation performance is greatly affected by the circuit conditions such as the diode part, the diameter of the bias post and the stem, and the diode position in the cavity, [18]–[21]. Fig. 8 shows the dependency of the oscillation frequency when the diode area is taken as a parameter. The bias post with a diameter of 0.6 mm in the *T*-band cavity is fixed throughout the experiments. With

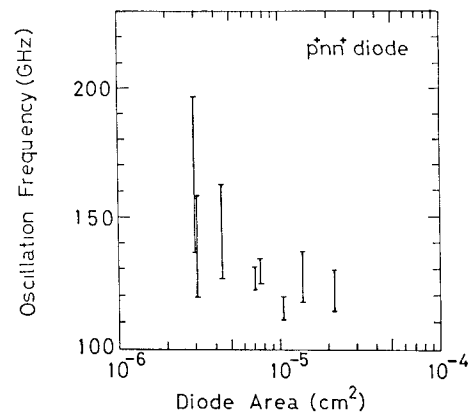

Fig. 8. Tuning characteristics in the oscillation frequency of the p^+-n-n^+ diode mounted in the *T*-band cavity as a parameter of the diode area.

reduction in the diode area, the oscillation frequency increases. This comes from the impedance matching between the circuit and the diode, and a smaller diode area seems to obtain a higher oscillation frequency. The oscillation characteristic of the two p^+-n-n^+ diode is shown in Figs. 9(a) and (b). The two bias posts with diameters of 0.3 and 0.6 mm in the *T*-band cavity are changed as shown in Fig. 9(a). A higher oscillation is obtained with a smaller diameter of the bias post. Fig. 9(b) shows the effect of circuit changes. The effect of the circuit parameter including the diode part is very complex. Hence a more detailed analysis will be necessary to obtain increased oscillation frequency and output power.

C. *Effect of Temperature on the Oscillation Performance*

The lowest pulsed input power of 2.1 W is obtained from the p^+-n-n^+ diode, and about 40 W can be applied to the p^+-n-n^+ diode. The tunnel current increases with an increase of the junction temperature. This is confirmed by the dc characteristics of the diode with $N_D \geq 8\times10^{17}$ cm^{-3}. Therefore, the TUNNETT oscillation manifests itself so that the output power increases with increasing junction temperature. The temperature effect is tested by a pulse oscillation experiment under a varying duty cycle. With increasing duty cycle, the output voltage of the detector increases. This oscillation performance coincides with the *I-V* characteristics and is different from that of the GaAs p-n IMPATT in which the output power is decreased as the duty cycle increases [22].

V. Discussion

The GaAs p^+-n and p^+-n-n^+ diodes with an impurity density N_D of the n layer higher than about 8×10^{17} cm^{-3} are confirmed experimentally to be oscillating in the TUNNETT mode; the fundamental oscillations at frequencies from about 100 up to 248 GHz are higher than those of the Si IMPATT [17]. Most of the bias voltage of the p^+-n-n^+ diode under experimentation was consumed only to extend the depletion layer with regard to the injection region but not for the drift region; consequently, the relatively larger bias current is needed to

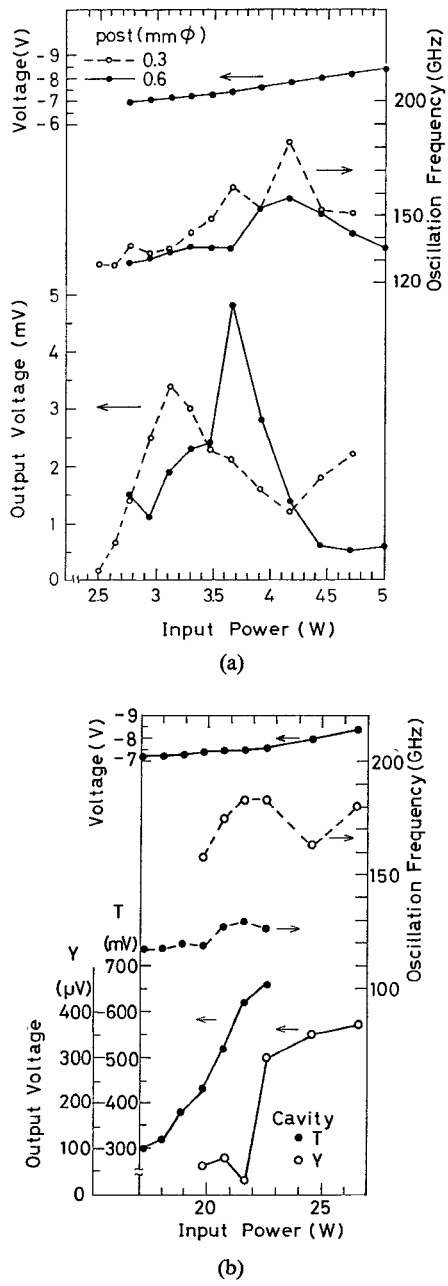

Fig. 9. (a) Oscillation characteristic of the p^+-n-n^+ diode mounted in the *T*-band cavity. The diameter of the bias post is changed as a parameter. (b) Oscillation characteristic of the p^+-n-n^+ diode mounted in the *T*- and *Y*-band cavities.

establish the high-field intensity in the drift region for the oscillation. This lower efficiency caused by the lower resistivity in the drift region will be improved with the introduction of the p^+-n^+-ν-n^+ structure. An optimum design of the diode will realize a much higher oscillation frequency with a higher output power from the TUNNETT diode.

VI. Conclusion

TUNNETT's with p^+-n and p^+-n-n^+ structures of GaAs are fabricated by a new LPE (TDM under CVP) method. The GaAs TUNNETT oscillation is found to be obtained when the doping density of the n layer is higher than about 8×10^{17} cm^{-3} and the electric-field intensity in the junction exceeds 1400~1500 kV/cm. The relation between the oscillation frequency and the bias current density are investigated by several waveguide circuits from 75 to 325 GHz, and it is made clear that the fundamental oscillations from about 100 up to 248 GHz are obtained. The lowest pulsed input power of 2.1 W and the bias current density of about 8×10^4 A/cm^2 are obtained from the p^+-n-n^+ diode, respectively.

Acknowledgment

The authors wish to thank Y. Takahashi and M. Sugawara for the cavity fabrication. They also wish to thank M. Iida and K. Shibuya for their aid in fabricating the parts of the waveguide circuit.

Diffusion in transit region can be avoided by the Gunn effect [23], which was also proposed for the IMPATT diode [24] and these were named as GUNNETT and GUNPATT by the author [25], respectively.

References

[1] J. Nishizawa and Y. Watanabe, "High frequency properties of the avalanching negative resistance diode," *Sci. Rep. Res. Inst. Tohoku Univ.*, B-(Comm.), vol. 10, no. 2, pp. 91–108, 1958.
[2] J. Nishizawa, "Tunnett diode," (in Japanese) *Ohyo Butsuri*, vol. 44, pp. 821–825, July 1975.
[3] J. Nishizawa, T. Ohmi, and M. S. Niranjian, "Avalanche induced dispersion in IMPATT diodes," *Solid-State Electron.*, vol. 21, no. 6, pp. 847–858, June 1978.
[4] T. Ishibashi, T. Makimura, and M. Ohmori, "Submillimeter wave silicon impatt diodes," IECE of Japan, Technical Group Meeting, MW 76–137 (in Japanese), Feb. 1977.
[5] T. Okabe, S. Takamiya, K. Okamoto, and J. Nishizawa, "Bulk oscillation by tunnel injection," presented at IEEE Int. Electron Device Meeting, Dec. 1968.
[6] J. Nishizawa and T. Ohmi, "Millimeter-wave oscillations of tunnel injection transit time (TUNNETT) diodes," in *Proc. 1973 European Microwave Conf.*, A. 10. 5.
[7] J. Nishizawa, T. Ohmi, and T. Sakai, "Millimeter-wave oscillation from Tunnett diode," in *Proc. 1974 European Microwave Conf.*, pp. 449–453.
[8] J. Nishizawa, K. Motoya, and Y. Okuno, "200 GHz TUNNETT diodes," in *Digest Tech. Papers 9th Conf. Solid-State Devices*, C-2-2, Aug. 1977.
[9] J. Nishizawa, K. Motoya, and Y. Okuno, "200 GHz TUNNETT diodes," *Japan. J. Appl. Phys.*, vol. 17, suppl. 17-1, pp. 167–172, 1978.
[10] J. Nishizawa, Y. Okuno, and H. Tadano, "Nearly perfect crystal growth of III-V compounds by the temperature difference method under controlled vapor pressure," *J. Cryst. Growth*, vol. 31, pp. 215–222, Dec. 1975.
[11] G. I. Haddad *et al.*, private communication.
[12] I. Shiota, K. Motoya, T. Ohmi, N. Miyamoto, and J. Nishizawa, "Auger characterization of chemically etched GaAs surfaces," *J. Electrochem. Soc.*, vol. 124, no. 1, pp. 155–157, Jan. 1977.
[13] E. O. Kane, "Theory of Tunneling," *J. Appl. Phys.*, vol. 32, no. 1, pp. 83–91, Jan. 1961.
[14] J. L. Moll, *Physics of Semiconductors.* New York: McGraw-Hill, 1964, ch. 12.
[15] P. N. Butcher, K. F. Hulme, and J. R. Morgan, "Dependence of peak current density on acceptor concentration in germanium tunnel diodes," *Solid-State Electron.*, vol. 5, pp. 358–360, 1962.
[16] T. Ishibashi, private communication.
[17] T. Ohmori, T. Ishibashi, and S. Ono, "Dependency of the highest oscillation frequency on junction diameter of IMPATT diodes," *IEEE Trans. Electron Devices*, vol. ED-24, pp. 1323–1329, Dec. 1977.
[18] M. Ino, T. Makimura and M. Ohmori, "Characteristics of millimeter-wave silicon impatt diodes," IECE of Japan, Technical Group Meeting, ED-49 (in Japanese), Oct. 1972.

[19] T. Ohmi and K. Motoya, "Millimeter wave oscillations from Tunnett diodes," IECE of Japan, Technical Group Meeting, ED 75-71 (in Japanese), Jan. 1976.
[20] M. Ohmori, T. Ishibashi, T. Makimura, and S. Ono, "Design of Si Impatt diodes for high-frequency operation," IECE, Japan, Technical Group Meeting, ED 75–72 (in Japanese), Jan. 1976.
[21] K. P. Weller, R. S. Ying, and D. H. Lee, "Millimeter IMPATT sources for the 130~170-GHz range," *IEEE Trans. Microwave Theory Tech.*, vol. MTT-24, pp. 738–743, Nov. 1976.
[22] K. Nishitani, O. Ishihara, H. Sawano, S. Mitsui, and K. Shirahata, "Characteristics of pulsed GaAs Impatt diodes," IECE of Japan, Technical Group Meeting, SSD 75–33 (in Japanese), Aug. 1975.
[23] J. Nishizawa, "Panel discussion of several problems on semiconductor oscillators," *Joint Convention Record of Four Institutes of Electrical Engineers*, Japan, pp. 121–144, Oct. 1971.
[24] Y. Hirachi, K. Kobayashi, K. Ogasawara, T. Hisatsugu, and Y. Toyama, "A new operation mode 'surfing mode' in high-low-type GaAs IMPATT's," *Tech. Dig. IEDM*, pp. 102–105, 1976.
[25] J. Nishizawa, "Progress of compound semiconductor devices," Penshi-Zairyo (in Japanese) pp. 18–22, May. 1974.

YIG Resonator Circuit with Isolator Property and Its Application to a Gunn Diode Oscillator

FUMIAKI OKADA, MEMBER, IEEE, KOICHI OHWI, STUDENT MEMBER, IEEE, AND YUKIO YOKOCHI

Abstract—**This paper presents the analysis and experiment of a newly developed YIG resonator circuit with isolator property, which is constructed with a YIG sphere, three coupling loops, and a 3-dB stripline directional coupler. This YIG circuit can be used advantageously as the tuning element of a magnetically tunable oscillator. The circuit has an advantage in preventing frequency pulling and the variation of output power level of the oscillator due to a change in load condition because of the resonator circuit having isolator property at the same time.**

The design procedure and experiment of a magnetically tunable Gunn diode oscillator with the YIG circuit is also shown. It has been confirmed that the YIG circuit when applied to a tunable oscillator is quite useful.

I. Introduction

OSCILLATION frequency and output power level of an oscillator are usually affected by wave reflection from its load. In order to prevent such influences, a buffer amplifier is used in lower microwave frequency bands and an isolator or a circulator are required in higher microwave bands. A YIG resonator is commonly used as a magnetically tunable element in a wide-band microwave sweep oscillator. Therefore it is necessary to use additionally a wide-band isolator or circulator in such a sweep oscillator. Since these are disadvantageous in size and cost, it is desirable to use a YIG element which has both resonator and isolator properties at the same time. One of the authors already reported such a kind of waveguide type YIG resonator circuit [1].

The waveguide YIG circuit makes use of circularly polarized RF magnetic field in the plane spaced $\lambda g/4$ from the narrow wall of the waveguide in order to obtain isolator property. This waveguide YIG circuit, however, is bulky and is inferior in size and operational frequency bandwidth.

Manuscript received May 29, 1978; revised July 28, 1978.

The authors are with the Department of Electrical Engineering, National Defense Academy, 1-10-20 Hashirimizu, Yokosuka, 239, Japan.

Thus a new YIG resonator circuit with isolator property has been developed which is constructed by using a YIG sphere resonator in conjunction with a 3-dB stripline directional coupler. This paper presents theoretical analysis and experimental confirmation of the new YIG resonator circuit with isolator property, followed by the design and experiment of a magnetically tunable Gunn diode oscillator using the YIG circuit. The value of the calculated scattering matrix of the YIG circuit agrees well with experimental results, and the magnetically tunable Gunn diode oscillator shows good improvement in frequency pulling and in eliminating output power level change due to load variation as compared with the usual magnetically tunable Gunn diode oscillator.

II. YIG Resonator Circuit with Isolator Property

Fig. 1 is a schematic of a magnetically tunable Gunn diode oscillator with a YIG resonator circuit having isolation properties. A YIG sphere is placed at the intersection of three semiloop axies. Two loops connected to ports 2′ and 3′ of a 3-dB directional coupler are placed orthogonally, similar to a nonreciprocal filter [2], [3]. The other semiloop at port 1 is placed on the opposite side of a metal plate for shielding. These loops are not coupled to each other when the YIG sphere is not resonant. Fig. 2 is the equivalent circuit in regards to ports 1, 2′, and 3′ of the YIG resonator part itself. The impedance matrix of the YIG resonator part is given by considering the equivalent circuit and a nonreciprocal phase shift, so the scattering matrix $[S_Y]$ of the equivalent circuit is obtained by converting this impedance matrix into a scattering matrix. Thus the obtained scattering matrix $[S_Y]$ is as follows:

0018-9480/78/1200-1035$00.75 ©1978 IEEE